

# Chargino Production and Decay in Photon-Photon-Collisions

T. MAYER, C. BLÖCHINGER<sup>1</sup>, F. FRANKE<sup>2</sup>, H. FRAAS<sup>3</sup>

*Institut für Theoretische Physik und Astrophysik, Universität Würzburg,  
D-97074 Würzburg, Germany*

## Abstract

We discuss the pair production of charginos in collisions of polarized photons  $\gamma\gamma \rightarrow \tilde{\chi}_i^+ \tilde{\chi}_i^-$ , ( $i = 1, 2$ ) and the subsequent leptonic decay of the lighter chargino  $\tilde{\chi}_1^+ \rightarrow \tilde{\chi}_1^0 e^+ \nu_e$  including the complete spin correlations. Analytical formulae are given for the polarization and the spin-spin correlations of the charginos. Since the production is a pure QED process the decay dynamics can be studied separately. For high energy photons from Compton backscattering of polarized laser pulses off polarized electron beams numerical results are presented for the cross section, the angular distribution and the forward-backward asymmetry of the decay positron. Finally we study the dependence on the gaugino mass parameter  $M_1$  and on the sneutrino mass for a gaugino-like MSSM scenario.

## 1 Introduction

From both a theoretical and a phenomenological point of view supersymmetry (SUSY) is the most attractive concept for new physics beyond the Standard Model. The first candidates for supersymmetric particles are expected to be discovered at the LHC. Then precision measurements are necessary to identify the specific supersymmetric scenario which is realized in nature and to determine the model parameters. Due to the clear signatures and the feasibility of polarized beams Linear Colliders offer outstanding possibilities to find SUSY particles and to study their properties [1]. Here charginos, the supersymmetric partners of the charged gauge and Higgs bosons, are of particular interest as they are expected to be light enough to be produced with comparably large cross sections at an  $e^+e^-$  collider. In the Minimal Supersymmetric Standard Model (MSSM) the production process is determined by the SUSY parameters  $M_2$ ,  $\mu$ ,  $\tan\beta$  and the sneutrino mass  $m_{\tilde{\nu}_e}$ , whereas the chargino decay into the lightest neutralino

<sup>1</sup>e-mail: bloechi@physik.uni-wuerzburg.de

<sup>2</sup>e-mail: fabian@physik.uni-wuerzburg.de

<sup>3</sup>e-mail: fraas@physik.uni-wuerzburg.de

$\tilde{\chi}_1^0$  which we assume to be the lightest supersymmetric particle (LSP) depends in addition on the gaugino mass parameter  $M_1$  and the mass  $m_{\tilde{e}_L}$  of the left selectron. The SUSY parameters can be determined with high precision in a combined analysis of neutralino and chargino pair production at an  $e^+e^-$  collider with polarized beams [2].

Besides for the  $e^+e^-$  option many studies for the  $\gamma\gamma$  mode of a Linear Collider have been performed with high luminosity polarized photon beams obtained by Compton-backscattering of laser pulses off the electron beams [3]. In the present paper we study chargino pair production  $\gamma\gamma \rightarrow \tilde{\chi}_i^+ \tilde{\chi}_i^-$  ( $i = 1, 2$ ) in photon collisions and the subsequent leptonic chargino decay. In our numerical analysis we focus on the decay of the light positive chargino  $\tilde{\chi}_1^+ \rightarrow \tilde{\chi}_1^0 e^+ \nu_e$ , but consider in the analytical formulae the complete spin correlations between the production and decay process.

Since the production is a pure QED process at tree level which depends only on the mass of the charginos the chargino decay mechanism can be studied separately in  $\gamma\gamma$  collisions. Provided the chargino mass has been measured and the energy spectrum and polarization of the high energy photons are well under control the production cross section and the polarization of the charginos are known and can be varied by suitable choice of the polarization of the laser photons and the converted electron beam. Then the direct measurement of the chargino decay branching ratios for the various decay channels may be useful for an analysis of the chargino system complementary to the  $e^+e^-$  mode where both production and decay are sensitive to the SUSY parameters.

This paper is organized as follows: In Sect. 2 we present the general spin density matrix formalism for the production of fermions with polarized photon beams and their subsequent decay. In order to analyze the influence of the fermion polarization on the forward-backward asymmetry of the decay product one needs the spin density production matrix which is given analytically in the  $\gamma\gamma$ -CMS for circularly polarized photons in Sect. 3. For two representative SUSY scenarios we present in Sect. 4 numerical results for the chargino production cross section, the branching ratio of the leptonic decay of the lighter chargino  $\tilde{\chi}_1^+$ , the angular distribution and the forward-backward asymmetry of the decay positron in the laboratory system (ee-CMS). Finally we study the dependence on the gaugino mass parameter  $M_1$  and on the sneutrino mass in a scenario with a gaugino-like LSP.

## 2 Helicity amplitudes and cross sections

The analytical formulae for the differential cross section of the combined process of chargino production by collisions of polarized photon beams

$$\gamma_1(k) + \gamma_2(k') \rightarrow \tilde{\chi}_k^-(p) + \tilde{\chi}_k^+(p') \quad (k = 1, 2) \quad (1)$$

and the leptonic decays

$$\tilde{\chi}_k^-(p) \rightarrow \tilde{\chi}_1^0(q_4) + e^-(q_5) + \bar{\nu}_e(q_6) \quad (2)$$

$$\tilde{\chi}_k^+(p') \rightarrow \tilde{\chi}_1^0(q_1) + e^+(q_2) + \nu_e(q_3) \quad (3)$$

with complete spin correlations are calculated using the same formalism as in [4] for  $e^+e^-$ -annihilation.

The production (1) is a pure QED process in leading order perturbation theory and depends only on the chargino mass  $m_k$ , which is expected to be measured in  $e^+e^-$  annihilation [1]. The helicity amplitudes corresponding to the Feynman diagrams in Fig. 1 are

$$T_{P,\alpha\beta}^{\lambda_i\lambda_j} = e^2 \bar{u}(p', \lambda_j) \left\{ \not{\epsilon}^{(\alpha)} \frac{Q + m_k}{Q^2 - m_k^2} \not{\epsilon}^{(\beta)} + \not{\epsilon}^{(\beta)} \frac{Q' + m_k}{Q'^2 - m_k^2} \not{\epsilon}^{(\alpha)} \right\} v(p, \lambda_i) \quad (4)$$

where  $p, \lambda_i$  ( $p', \lambda_j$ ) are the momenta and helicities of the chargino  $\tilde{\chi}_k^-$  ( $\tilde{\chi}_k^+$ ). The exchanged charginos have momenta  $Q = k - p$  and  $Q' = k' - p$  and the polarization vectors of the photons with momenta  $k, k'$  are denoted by  $\epsilon^{(\beta)}$  and  $\epsilon'^{(\alpha)}$ , respectively. In the following we consider only right ( $\alpha, \beta = 1$ ) or left ( $\alpha, \beta = -1$ ) circularly polarized photons.

The amplitude for production and decay reads

$$T_{\alpha\beta} = \Delta(\tilde{\chi}_k^-) \Delta(\tilde{\chi}_k^+) \sum_{\lambda_i, \lambda_j} T_{P,\alpha\beta}^{\lambda_i\lambda_j} T_D^{\lambda_i} T_D^{\lambda_j} \quad (5)$$

with the propagators of the charginos with mass  $m_k$  and width  $\Gamma_k$

$$\Delta(\tilde{\chi}_k^-) = \frac{1}{p^2 - m_k^2 + im_k\Gamma_k} \quad (6)$$

$$\Delta(\tilde{\chi}_k^+) = \frac{1}{p'^2 - m_k^2 + im_k\Gamma_k}. \quad (7)$$

For these propagators we use the narrow width approximation.

The helicity amplitudes  $T_D^{\lambda_i}(\tilde{\chi}_k^-)$  and  $T_D^{\lambda_j}(\tilde{\chi}_k^+)$  for the leptonic decays (2) and (3) of the charginos via  $W^\pm, \tilde{e}_L$  and  $\tilde{\nu}_e$  exchange (Fig. 2) are given in [4, 5]. They depend on the gaugino mass parameters  $M_1, M_2$ , the higgsino mass parameter  $\mu$ , the ratio  $\tan\beta$  of the vacuum expectation values of the neutral Higgs fields and the left selectron and the sneutrino mass.

The differential cross section for production and subsequent decay of both charginos in the  $\gamma\gamma$ -CMS is

$$d\sigma_{\alpha\beta} = \frac{1}{8E^2} |T_{\alpha\beta}|^2 (2\pi)^4 \delta^4(k + k' - \sum_i q_i) d\text{lips}(q_1, q_2, q_3, q_4, q_5, q_6) \quad (8)$$

where  $E$  is the energy of the photon beam and  $d\text{lips}(q_1, q_2, q_3, q_4, q_5, q_6)$  denotes the Lorentz invariant phase space element.

The amplitude squared (using the sum convention)

$$|T_{\alpha\beta}|^2 = |\Delta(\tilde{\chi}_k^-)|^2 |\Delta(\tilde{\chi}_k^+)|^2 \rho_{P,\alpha\beta}^{\lambda_i\lambda_j, \lambda'_i\lambda'_j} \rho_D^{\lambda'_i\lambda_i}(\tilde{\chi}_k^-) \rho_D^{\lambda'_j\lambda_j}(\tilde{\chi}_k^+) \quad (9)$$

is composed of the unnormalized spin density production matrix

$$\rho_{P,\alpha\beta}^{\lambda_i\lambda_j,\lambda'_i\lambda'_j} = T_{P,\alpha\beta}^{\lambda_i\lambda_j} T_{P,\alpha\beta}^{\lambda'_i\lambda'_j*} \quad (10)$$

and the decay matrices

$$\rho_D^{\lambda'_i\lambda_i}(\tilde{\chi}_k^-) = T_D^{\lambda_i} T_D^{\lambda'_i*} \quad \rho_D^{\lambda'_j\lambda_j}(\tilde{\chi}_k^+) = T_D^{\lambda_j} T_D^{\lambda'_j*} . \quad (11)$$

Introducing a suitable set of polarization vectors  $s^a$  ( $s^b$ ) for the chargino  $\tilde{\chi}_k^-$  ( $\tilde{\chi}_k^+$ ) one can expand the density matrices (10), (11) in terms of Pauli matrices [6]

$$\rho_{P,\alpha\beta}^{\lambda_i\lambda_j,\lambda'_i\lambda'_j} = \delta_{\lambda_i\lambda'_i}\delta_{\lambda_j\lambda'_j}P_{\alpha\beta} + \delta_{\lambda_j\lambda'_j}\sigma_{\lambda_i\lambda'_i}^a\Sigma_{P,\alpha\beta}^a + \delta_{\lambda_i\lambda'_i}\sigma_{\lambda_j\lambda'_j}^b\Sigma_{P,\alpha\beta}^b \quad (12)$$

$$+ \sigma_{\lambda_i\lambda'_i}^a\sigma_{\lambda_j\lambda'_j}^b\Sigma_{P,\alpha\beta}^{ab} \quad (13)$$

$$\rho_D^{\lambda'_i\lambda_i}(\tilde{\chi}_k^-) = \delta_{\lambda'_i\lambda_i}D_i + \sigma_{\lambda'_i\lambda_i}^a\Sigma_D^a \quad (14)$$

$$\rho_D^{\lambda'_j\lambda_j}(\tilde{\chi}_k^+) = \delta_{\lambda'_j\lambda_j}D_j + \sigma_{\lambda'_j\lambda_j}^b\Sigma_D^b \quad (15)$$

and obtains

$$|T_{\alpha\beta}|^2 = 4|\Delta(\tilde{\chi}_k^-)|^2|\Delta(\tilde{\chi}_k^+)|^2(P_{\alpha\beta}D_iD_j + D_j\Sigma_{P,\alpha\beta}^a\Sigma_D^a + D_i\Sigma_{P,\alpha\beta}^b\Sigma_D^b + \Sigma_{P,\alpha\beta}^{ab}\Sigma_D^a\Sigma_D^b) . \quad (16)$$

The ratio  $\Sigma_{P,\alpha\beta}^a/P_{\alpha\beta}$  ( $\Sigma_{P,\alpha\beta}^b/P_{\alpha\beta}$ ) describes the polarization of the chargino  $\tilde{\chi}_k^-$  ( $\tilde{\chi}_k^+$ ).  $\Sigma_{P,\alpha\beta}^{ab}$  originates from spin-spin correlations between both charginos. The analytical formulae for the quantities  $P_{\alpha\beta}$ ,  $\Sigma_{P,\alpha\beta}^a$ ,  $\Sigma_{P,\alpha\beta}^b$  and  $\Sigma_{P,\alpha\beta}^{ab}$  are given in the next section. Analytical expressions for the decay matrices for the leptonic decays (2) and (3) can be found in [4, 5].

If the decay of only one of the charginos,  $\tilde{\chi}_k^+(p') \rightarrow \tilde{\chi}_1^0(q_1)e^+(q_2)\nu_e(q_3)$ , is considered it is  $D_i = 1$ ,  $\Sigma_D^a = 0$  and  $\Delta(\tilde{\chi}_k^-) = 1$  in (16). Replacing the phase space element in (8) by  $d\text{lips}(p, q_1, q_2, q_3)$  and integrating over the phase space of the LSP and the neutrino lead to the cross section  $d\sigma_{e,\alpha\beta}$  of the decay positron. With the substitution  $|T_{\alpha\beta}|^2 = 4P_{\alpha\beta}$  in (8) and the phase space element  $d\text{lips}(p, p')$  one obtains the chargino production cross section  $d\sigma_{P,\alpha\beta}$ .

The optimal source of high energy polarized photon beams is Compton backscattering of intense laser pulses off one of the beams of a linear collider in the  $e^-e^-$  mode. The energy distribution  $P(y)$  and the mean helicity  $\lambda(y)$  strongly depend on the polarizations  $\lambda_L$  of the laser photons and  $\lambda_e$  of the converted electrons. The analytical formulas can be found in [3, 7]. To obtain the chargino production cross section  $d\sigma_P(s_{\gamma\gamma})/d\cos\theta$  for circularly polarized photons one has to weight the cross section  $d\sigma_{P,\alpha\beta}(s_{\gamma\gamma})/d\cos\theta$  with the mean helicity  $\lambda(y_1)$  and  $\lambda(y_2)$  of both beams

$$\frac{d\sigma_P(s_{\gamma\gamma})}{d\cos\theta} = \frac{1}{4} \sum_{\alpha,\beta=\pm 1} (1 + \alpha\lambda(y_1))(1 + \beta\lambda(y_2)) \frac{d\sigma_{P,\alpha\beta}(s_{\gamma\gamma})}{d\cos\theta} . \quad (17)$$

Here  $y_1 = E_{\gamma_1}/E_{e_1}$  ( $y_2 = E_{\gamma_2}/E_{e_2}$ ) is the ratio of the energies of the high energy photons  $\gamma_1(k)$  ( $\gamma_2(k')$ ) and of the energies of the respective converted electrons  $e_1$  ( $e_2$ ). Convoluting the cross section (17) with the energy distribution  $P(y_1)$  and  $P(y_2)$  of the high energy photons one obtains the differential cross section in the laboratory frame (ee-CMS) [8]

$$\frac{d\sigma_p(s_{ee})}{d\cos\theta^L} = \int P(y_1)P(y_2) \frac{d\sigma_p}{d\cos\theta}(\cos\theta(\cos\theta^L), s_{\gamma\gamma} = y_1 y_2 s_{ee}) \frac{d\cos\theta}{d\cos\theta^L} dy_1 dy_2. \quad (18)$$

As indicated in (18) the scattering angle  $\theta$  in the  $\gamma\gamma$ -CMS has to be expressed by the scattering angle  $\theta^L$  in the ee-CMS:

$$\cos\theta = \frac{y_2(1 + \cos\theta^L) - y_1(1 - \cos\theta^L)}{y_2(1 + \cos\theta^L) + y_1(1 - \cos\theta^L)}. \quad (19)$$

Weighting the total cross section  $d\sigma_p(s_{\gamma\gamma})$  as in (17) with the mean helicities one obtains the total cross section  $d\sigma_p(s_{ee})$  in the ee-CMS by the convolution [9]

$$\sigma_p(s_{ee}) = \int P(y_1)P(y_2)\sigma_p(s_{\gamma\gamma} = y_1 y_2 s_{ee}) dy_1 dy_2 \quad (20)$$

The same procedure applies to the differential cross section  $d\sigma_e(s_{ee})/d\cos\theta_{e^+}^L$  and the total cross section  $\sigma_e(s_{ee})$  of the positrons from chargino production and subsequent leptonic decay.

In the laboratory system (ee-CMS) it is  $E_1 = E_2 = E$  and  $s_{\gamma\gamma} = y_1 y_2 s_{ee}$  with  $\sqrt{s_{ee}} = 2E$ . To prevent  $e^+e^-$  pair production by scattering of the photon beam and the laser beam the ratio  $y$  has to be adjusted to  $y \leq 0.83$  which leads to  $\sqrt{s_{\gamma\gamma}^{max}} = 0.83\sqrt{s_{ee}}$ .

### 3 The spin-density production matrix

In this section we give the analytical formulae for the quantities  $P_{\alpha\beta}$ ,  $\Sigma_{P,\alpha\beta}^a$ ,  $\Sigma_{P,\alpha\beta}^b$ ,  $\Sigma_{P,\alpha\beta}^{ab}$  in (16) for production of charged spin- $\frac{1}{2}$  fermions in collisions of circularly polarized photons. For our study of the combined process of production and decay it is convenient to choose a coordinate frame where the momenta are given by

$$k^\mu = E(1, -\sin\theta, 0, \cos\theta) \quad (21)$$

$$k'^\mu = E(1, \sin\theta, 0, -\cos\theta) \quad (22)$$

$$p^\mu = (E, 0, 0, -q) \quad (23)$$

$$p'^\mu = (E, 0, 0, q) \quad (24)$$

with  $q = |\vec{p}| = |\vec{p}'|$ . For the chargino  $\tilde{\chi}_k^-$  ( $\tilde{\chi}_k^+$ ) with momentum  $p$  ( $p'$ ) and mass  $m_k$  we introduce three space-like polarization vectors  $s^{a\mu}$  ( $s'^{b\mu}$ ) ( $a, b = 1, 2, 3$ ), which together with  $\frac{p^\mu}{m_k}$  ( $\frac{p'^\mu}{m_k}$ ) form an orthonormal set

$$s^{1\mu} = (0, -1, 0, 0) \quad (25)$$

$$s^{2\mu} = (0, 0, 1, 0) \quad (26)$$

$$s^{3\mu} = \frac{1}{m_k}(q, 0, 0, -E) \quad (27)$$

$$s'^{1\mu} = (0, 1, 0, 0) \quad (28)$$

$$s'^{2\mu} = (0, 0, 1, 0) \quad (29)$$

$$s'^{3\mu} = \frac{1}{m_k}(q, 0, 0, E) \quad (30)$$

Here  $s^3$  ( $s'^3$ ) denotes the longitudinal polarization,  $s^1$  ( $s'^1$ ) the transverse polarization in the production plane and  $s^2$  ( $s'^2$ ) the transverse polarization perpendicular to the production plane. With our choice of the coordinate frame the polarization vectors for circularly polarized photons are

$$\varepsilon_\mu^{(\alpha)}(\gamma_2) = \frac{1}{\sqrt{2}}(0, -\alpha \cos \theta, i, -\alpha \sin \theta) \quad (31)$$

$$\varepsilon_\mu^{(\beta)}(\gamma_1) = \frac{1}{\sqrt{2}}(0, \beta \cos \theta, i, \beta \sin \theta) \quad (32)$$

with  $\alpha, \beta = +1$  ( $\alpha, \beta = -1$ ) for right (left) circularly polarized photons.

The expression  $P_{\alpha\beta}$  is independent of the chargino polarization and reads

$$P_{\alpha\beta} = C\{(1 + \alpha\beta)m_k^2(2E^2 - m_k^2) + (1 - \alpha\beta)q^2 \sin^2 \theta(2E^2 - q^2 \sin^2 \theta)\} \quad (33)$$

with

$$C = \frac{e^4}{(E^2 - q^2 \cos^2 \theta)^2}. \quad (34)$$

The contributions  $\Sigma_{P,\alpha\beta}^a$  of the polarization of the chargino  $\tilde{\chi}_k^-$  are

$$\Sigma_{P,\alpha\beta}^1 = -2C(\alpha - \beta)Eq^2 m_k \sin^3 \theta \quad (35)$$

$$\Sigma_{P,\alpha\beta}^2 = 0 \quad (36)$$

$$\Sigma_{P,\alpha\beta}^3 = 2CEq\{(\alpha + \beta)m_k^2 + (\alpha - \beta)Eq \sin^2 \theta \cos \theta\}. \quad (37)$$

To obtain the contributions  $\Sigma_{P,\alpha\beta}^b$  from the polarization of  $\tilde{\chi}_k^+$  one has to exchange  $\alpha$  and  $\beta$  in (35) – (36).

For the quantities  $\Sigma_{P,\alpha\beta}^{ab}$  describing the spin-spin-correlations between both charginos one obtains

$$\Sigma_{P,\alpha\beta}^{11} = C\{(1 + \alpha\beta)m_k^4 - (1 - \alpha\beta)q^2(E^2 + m_k^2) \sin^4 \theta\} \quad (38)$$

$$\Sigma_{P,\alpha\beta}^{22} = -C\{(1 + \alpha\beta)m_k^4 + (1 - \alpha\beta)q^4 \sin^4 \theta\} \quad (39)$$

$$\Sigma_{P,\alpha\beta}^{33} = C\{(1 + \alpha\beta)m_k^2(2E^2 - m_k^2) - (1 - \alpha\beta)q^2 \sin^2 \theta [2E^2 - (E^2 + m_k^2) \sin^2 \theta]\} \quad (40)$$

$$\Sigma_{P,\alpha\beta}^{13} = C(1 - \alpha\beta)2Eq^2 m_k \sin^3 \theta \cos \theta = \Sigma_{P,\alpha\beta}^{31} \quad (41)$$

$$\Sigma_{P,\alpha\beta}^{12} = 0 = \Sigma_{P,\alpha\beta}^{21} = \Sigma_{P,\alpha\beta}^{23} = \Sigma_{P,\alpha\beta}^{32}. \quad (42)$$

For unpolarized photon beams it is  $\alpha = 0$  or/and  $\beta = 0$ . If both beams are unpolarized the charginos are also unpolarized and the spin correlations between production and decay of one of the charginos vanish. If, however, the decay of both charginos is considered the spin-spin correlations (38)-(42) are crucial for the distribution of the opening angle between the decay products of both of them.

From  $P_{\alpha\beta}$  (33) one obtains the differential cross section for production of charged spin- $\frac{1}{2}$ -fermions with polarized photon beams:

$$\frac{d\sigma_{p,\alpha\beta}}{d\cos\theta} = \frac{q}{32\pi E^3} P_{\alpha\beta} \quad (43)$$

and the total cross section

$$\begin{aligned} \sigma_{p,\alpha\beta} = & \frac{e^4}{16\pi E^6} \left\{ [m_k^2(2E^2 - m_k^2) + 2E^4(1 - \alpha\beta)] \ln \frac{E+q}{m_k} \right. \\ & \left. + Eq[2E^2 - m_k^2 - 3E^2(1 - \alpha\beta)] \right\}. \end{aligned} \quad (44)$$

Both the differential and the total production cross sections are sensitive to photon polarization only if both beams are polarized. In addition the cross section does not change by replacing both  $\alpha \rightarrow -\alpha$  and  $\beta \rightarrow -\beta$ .

## 4 Numerical results

In the MSSM the masses and couplings of the charginos and neutralinos are determined by the parameters  $M_1$ ,  $M_2$ ,  $\mu$  and  $\tan\beta$  with  $M_1$  usually fixed by the GUT relation  $M_1 = \frac{5}{3}M_2 \tan^2\theta_W$ . The parameters are chosen to be real assuming CP-conservation.

We study pair production and leptonic decay of the lighter chargino in two representative scenarios A [10] and B with the parameters given in Table 1. In scenario A both the lighter chargino and the LSP are gaugino-like while in scenario B  $\tilde{\chi}_1^\pm$  and  $\tilde{\chi}_1^0$  are Higgsino-like. The choice of the slepton masses corresponds to a common scalar mass  $m_0 = 100$  GeV. The masses of  $\tilde{\nu}_e$  and  $\tilde{e}_L$  are at tree level connected by the  $SU(2)_L$  relation

$$m_{\tilde{e}_L}^2 = m_{\tilde{\nu}_e}^2 - m_W^2 \cos 2\beta. \quad (45)$$

In sections 4.3 and 4.4 we study the dependence of the cross section  $\sigma_e$  and of the forward-backward asymmetry on  $M_1$  and  $m_{\tilde{\nu}_e}$ .

### 4.1 Cross sections for chargino production

The chargino production process is in leading order perturbation theory completely model independent and only determined by the mass  $m_k$  and the charge of the produced fermions. In Fig. 3 we show the convoluted cross section  $\sigma_p$

for  $m_k = 128$  GeV and for polarizations  $\lambda_c = 0, \pm 0.85$  of the converted electrons and for unpolarized or right circularly polarized ( $\lambda_L = 1$ ) laser photons. For high energies one obtains the highest cross section for  $(\lambda_{c_1}, \lambda_{L_1}) = (0.85, 0)$  and  $(\lambda_{c_2}, \lambda_{L_2}) = (-0.85, 0)$  whereas for lower energies  $\sqrt{s_{ee}} \leq 600$  GeV the polarizations  $(\lambda_{c_1}, \lambda_{L_1}) = (0.85, -1)$ ,  $(\lambda_{c_2}, \lambda_{L_2}) = (0.85, -1)$  are favored. For this combination of polarizations the dependence of  $\sigma_p$  on the chargino mass at  $\sqrt{s_{ee}} = 500$  GeV is shown in Fig. 4. As a pure QED process the production cross section is forward-backward symmetric. The shape of the angular distribution depicted in Fig. 5 for  $\sqrt{s} = 500$  GeV, however, depends on the polarization configurations. For  $(\lambda_{c_1}, \lambda_{L_1}) = (0.85, 0)$ ,  $(\lambda_{c_2}, \lambda_{L_2}) = (0.85, 0)$  the forward and backward direction is favored, whereas for  $(\lambda_{c_1}, \lambda_{L_1}) = (0.85, 0)$ ,  $(\lambda_{c_2}, \lambda_{L_2}) = (-0.85, 0)$  the angular distribution is nearly isotropic.

For polarized laser photons and electrons one can define diverse polarization asymmetries. As an example we show in Fig. 6 at  $\sqrt{s_{ee}} = 500$  GeV and  $\sqrt{s_{ee}} = 800$  GeV the dependence on the fermion (chargino) mass of the polarization asymmetry

$$A_{\text{Pol}} = \frac{\sigma_p(\lambda_{c_1}, \lambda_{L_1}, \lambda_{c_2}, \lambda_{L_2}) - \sigma_p(\lambda_{c_1}, \lambda_{L_1}, \lambda_{c_2}, -\lambda_{L_2})}{\sigma_p(\lambda_{c_1}, \lambda_{L_1}, \lambda_{c_2}, \lambda_{L_2}) + \sigma_p(\lambda_{c_1}, \lambda_{L_1}, \lambda_{c_2}, -\lambda_{L_2})} \quad (46)$$

with the polarization of only one laser pulse flipped.

## 4.2 Cross section and forward-backward asymmetry of the decay leptons

The total cross section of the decay leptons given in Table 2 for  $\sqrt{s_{ee}} = 500$  GeV and  $\sqrt{s_{ee}} = 800$  GeV and polarizations  $(\lambda_{c_1}, \lambda_{L_1}) = (0.85, 0)$ ,  $(\lambda_{c_2}, \lambda_{L_2}) = (-0.85, 0)$  is not affected by spin correlations and factorizes into the chargino production cross section and the leptonic branching ratio. Since, however, the angular distribution of the decay products is sensitive to the polarization of the parent particle [4], the forward-backward asymmetry

$$A_{\text{FB}} = \frac{\sigma_e(\cos \theta_{e^+} > 0) - \sigma_e(\cos \theta_{e^+} < 0)}{\sigma_e(\cos \theta_{e^+} > 0) + \sigma_e(\cos \theta_{e^+} < 0)} \quad (47)$$

of the positrons from the decay  $\tilde{\chi}_1^+ \rightarrow \tilde{\chi}_1^0 e^+ \nu_e$  may be quite large. Since the production process and the transverse polarization of the charginos  $\Sigma_{P,\alpha\beta}^1$  (35) is forward-backward symmetric  $A_{\text{FB}}$  will be largest for forward-backward antisymmetric longitudinal polarization  $\Sigma_{P,\alpha\beta}^3$ . For monochromatic photons this is the case for opposite circular polarization ( $\alpha = -\beta = \pm 1$ ) of both beams, whereas for unpolarized photon beams or beams with the same polarization  $\alpha = \beta$  corresponding to  $(\lambda_{c_1}, \lambda_{L_1}) = (\lambda_{c_2}, \lambda_{L_2})$ , the longitudinal polarization  $\Sigma_{P,\alpha\beta}^3$  is forward-backward symmetric and the forward-backward asymmetry  $A_{\text{FB}} = 0$  vanishes. Analogously, the case of Compton backscattering of laser pulses off oppositely polarized electron beams ( $\lambda_{c_1} = -\lambda_{c_2} = 0.85$ ) and unpolarized laser photons ( $\lambda_{L_1} = \lambda_{L_2} = 0$ ) results in the largest forward-backward asymmetry of



the decay leptons since for this combination the high energy photons are polarized with mean helicities  $\lambda(y_1) > 0$  and  $\lambda(y_2) < 0$  [7]. Near threshold the spin correlations between production and decay are strongest at the expense of the cross section, which is largest for the combination  $\lambda_{c_1} = \lambda_{c_2} = 0.85$  and  $\lambda_{L_1} = \lambda_{L_2} = -1$  (Fig. 3).

In Figs. 7 and 8 we show the angular distributions for  $\lambda_{c_1} = -\lambda_{c_2} = 0.85$ ,  $\lambda_{L_1} = \lambda_{L_2} = 0$  at  $\sqrt{s_{ee}} = 500$  GeV and  $\sqrt{s_{ee}} = 800$  GeV in scenario A and scenario B. The lepton angular distribution sensitively depends on the mixing character of the chargino and the neutralino. In the gaugino-like scenario A it exhibits large asymmetries,  $A_{FB} = -18\%$  for  $\sqrt{s_{ee}} = 500$  GeV and  $A_{FB} = -12\%$  for  $\sqrt{s_{ee}} = 800$  GeV, whereas in the higgsino-like scenario B the angular distribution is nearly symmetric with  $A_{FB} = 0.83\%$  for  $\sqrt{s_{ee}} = 500$  GeV and  $A_{FB} = 0.36\%$  for  $\sqrt{s_{ee}} = 800$  GeV (Table 2).

Since the total cross section  $\sigma_e$  factorizes into the production cross section  $\sigma_p$  and the branching ratio of the chargino decay, the polarization asymmetries of  $\sigma_e$  are identical to those of  $\sigma_p$  and independent of the chargino decay.

### 4.3 $M_1$ -Dependence

Several studies analyze the determination of the gaugino mass parameter  $M_1$  via production and subsequent leptonic decay of neutralinos or selectrons in  $e^+e^-$  annihilation [11]–[16], via selectron production in  $e^-e^-$  scattering [16, 17] or via associated selectron neutralino (LSP) production in  $e\gamma$  scattering processes [18, 19]. In all these processes the  $M_1$  dependence of the cross sections of the decay leptons, their polarization and forward-backward asymmetries result from a complex interplay of the  $M_1$  dependence of the respective production and decay mechanism.

In the process investigated here only the decay of the charginos contributes to the  $M_1$  dependence of the cross section  $\sigma_e$  and to the forward-backward asymmetry  $A_{FB}$  of the decay leptons. In the following we study the  $M_1$  dependence of  $\sigma_e$  and  $A_{FB}$  fixing the other parameters as in scenario A and B.

The decay observables are affected by the  $M_1$  dependence of both the LSP mass  $m_{\tilde{\chi}_1^0}$  and the relevant couplings displayed in Figs. 9 – 11. The  $M_1$  dependence of  $m_{\tilde{\chi}_1^0}$  is very similar in both scenarios and shows a strong variation for  $M_1 < 150$  GeV. The variation of the couplings with  $M_1$ , however, sensitively depends on the mixing character of the chargino  $\tilde{\chi}_1^\pm$  and is in both scenarios very pronounced for  $M_1 < 170$  GeV.

Since the  $M_1$  dependence of  $\sigma_e$  is exclusively determined by the decay we show in Fig. 12 the branching ratio for the decay channel  $\tilde{\chi}_1^+ \rightarrow \tilde{\chi}_1^0 e^+ \nu_e$  for  $M_2 = 152$  GeV,  $\mu = 316$  GeV corresponding to the gaugino-like scenario A. For  $M_1 < 50$  GeV the two body-decay  $\tilde{\chi}_1^+ \rightarrow \tilde{\chi}_1^0 W^+$  is kinematically allowed and the leptonic branching ratio of the chargino  $BR(\tilde{\chi}_1^+ \rightarrow \tilde{\chi}_1^0 e^+ \nu_e) \approx BR(\tilde{\chi}_1^+ \rightarrow \tilde{\chi}_1^0 W^+) \times BR(W^+ \rightarrow e^+ \nu_e)$  is nearly independent of  $M_1$ . Between  $M_1 = 50$  GeV and  $M_1 = 100$  GeV the branching ratio and consequently the cross section  $\sigma_e = \sigma_p \times BR(\tilde{\chi}_1^+ \rightarrow \tilde{\chi}_1^0 e^+ \nu_e)$  varies by a factor 1.5.

Provided that the parameter  $M_2$  is measured in chargino production in  $e^+e^-$  annihilation the  $\gamma\gamma$  mode of a Linear Collider provides a test of the GUT relation between  $M_1$  and  $M_2$ . The forward-backward asymmetry of the decay positron (Fig. 13), however, turns out to be much more sensitive on  $M_1$  than the cross section  $\sigma_e$ . It changes monotonously from 19% to 5% in the region  $50 \text{ GeV} < M_1 < 150 \text{ GeV}$ .

For  $M_2 = 370 \text{ GeV}$ ,  $\mu = 125 \text{ GeV}$  corresponding to the higgsino-like scenario B the branching ratio and the cross section  $\sigma_e$  is nearly independent of  $M_1$ . In this scenario the forward-backward asymmetry is smaller than 1% for all values of  $M_1$ .

#### 4.4 Sneutrino mass dependence

In [20] methods have been proposed to determine the sneutrino mass from chargino pair production and decay in  $e^+e^-$ -annihilation. If the chargino has a large gaugino component sneutrino and selectron exchange strongly influence the leptonic branching ratio and the lepton angular distribution. In this section we study the  $m_{\tilde{\nu}_e}$  dependence of the cross section  $\sigma_e$  and the forward-backward asymmetry of the decay lepton assuming the  $SU(2)_L$  relation (45) for  $m_{\tilde{e}_L}$ . All other parameters are fixed as in scenario A.

As a function of the sneutrino mass we show in Fig. 14 the branching ratio  $BR(\tilde{\chi}_1^+ \rightarrow \tilde{\chi}_1^0 e^+ \nu_e)$  and in Fig. 15 the forward-backward asymmetry for  $\sqrt{s_{ee}} = 500 \text{ GeV}$  and beam polarizations  $(\lambda_{c_1}, \lambda_{L_1}) = (0.85, 0)$  and  $(\lambda_{c_2}, \lambda_{L_2}) = (-0.85, 0)$ . These polarization configurations result in the largest forward-backward asymmetry. The cross section shows a pronounced  $m_{\tilde{\nu}_e}$  dependence for  $m_{\tilde{\nu}_e} \lesssim 250 \text{ GeV}$  whereas the forward-backward asymmetry exhibits an appreciable  $m_{\tilde{\nu}_e}$  dependence up to  $m_{\tilde{\nu}_e} \sim 400 \text{ GeV}$ , which is considerably beyond the kinematical limit for sneutrino pair production in  $e^+e^-$ -annihilation at  $\sqrt{s_{ee}} = 500 \text{ GeV}$ .

For  $m_{\tilde{\nu}_e} < m_{\tilde{\chi}_1^+}$  the two-body decays  $\tilde{\chi}_1^+ \rightarrow l^+ \tilde{\nu}_l$ ,  $l = (e, \mu)$  and eventually  $l = (e, \mu, \tau)$  are dominating. Since for our set of parameters the sneutrino decays completely invisible via  $\tilde{\nu}_l \rightarrow \tilde{\chi}_1^0 \nu_l$  the branching ratio for  $\tilde{\chi}_1^+ \rightarrow \tilde{\chi}_1^0 e^+ \nu_e$  is given by that for the two-body decay into positron and sneutrino and therefore independent of the sneutrino mass.

For  $m_{\tilde{\nu}_e} > m_{\tilde{\chi}_1^+}$ , however, the  $m_{\tilde{\nu}_e}$  dependence of both the cross section and the forward-backward asymmetry is free of any ambiguities. With increasing sneutrino mass the contributions from  $\tilde{\nu}_e$  and  $\tilde{e}_L$  exchange are more and more suppressed so that finally only the contribution from  $W$ -exchange survives. We conclude that measuring the forward-backward asymmetry with suitably polarized beams is a useful method for the determination of the sneutrino mass. For a quantitative evaluation of the accuracy Monte Carlo studies would be necessary.

## 5 Conclusion

Pair production of charginos with subsequent decay in photon-photon collisions allows to study the decay mechanism separately from production. We have presented analytical formulae for the polarization and the spin-spin correlations of fermions produced in collisions of circularly polarized photon beams.

For high energy photons from Compton backscattering of polarized laser pulses off polarized electron beams we calculated the production cross section of the lighter chargino and the cross section, the angular distribution and the forward-backward asymmetry of the positron from the leptonic  $\tilde{\chi}_1^+$  decay. We have shown that for gaugino-like chargino and LSP the cross section and particularly the forward-backward asymmetry of the decay leptons is sensitive to the gaugino mass parameter  $M_1$  and to the sneutrino mass and allows to constrain them. Contrary to chargino production in electron-positron annihilation neither the dependence on the gaugino mass parameter  $M_1$  nor the dependence on the sneutrino mass of the cross section and the forward-backward asymmetry show ambiguities above the threshold for two-particle decay of the chargino.

## Acknowledgements

This work was supported by the Deutsche Forschungsgemeinschaft, contract FR 1064/4-1 and the Bundesministerium für Bildung und Forschung, contract 05 HT9WWa 9.

## References

- [1] TESLA Technical Design Report, Part III: Physics at an  $e^+e^-$  Linear Collider, eds. R. D. Heuer, D. Miller, F. Richard, P. Zerwas, Hamburg, March 2001, DESY 2001-011, ECFA 2001-209, TESLA Report 2001-23, TESLA FEL-2001-05.
- [2] S.Y. Choi, J. Kalinowski, G. Moortgat-Pick, P. Zerwas, Eur. Phys. J. **C22** (2001) 563, *and references therein*.
- [3] R. Badelek et al., *The photon collider at TESLA*, in: TESLA Technical Design Report, Part VI: Appendices, ed. R. Klanner, Hamburg, March 2001, DESY 2001-011, ECFA 2001-209, TESLA Report 2001-23, TESLA FEL-2001-05, *and references therein*.
- [4] G. Moortgat-Pick, H. Fraas, A. Bartl, W. Majerotto, Eur. Phys. J. **C7** (1999) 113.
- [5] S. Y. Choi, A. Djouadi, H. Dreiner, J. Kalinowski, P. M. Zerwas, Eur. Phys. J. **C7** 1999 123.
- [6] H. E. Haber, Proceedings of the 21st SLAC Summer Institute on Particle Physics, eds. L. DePorcel, Ch. Dunwoodie, Stanford 1993, p. 231.

- [7] I. F. Ginzburg, G. L. Kotkin, S. L. Panfil, V. G. Serbo, V. I. Telnov, Nucl. Inst. Meth. **A219** (1984) 5.
- [8] T. Kon, K. Nakamura, T. Kobayashi, Z. Phys. **C45** (1990) 567.
- [9] S. Hesselbach, H. Fraas, Phys. Rev. **D55** (1997) 1343.
- [10] S. Ambrosanio, G. A. Blair, P. Zerwas, ECFA-DESY LC-Workshop, 1998.
- [11] J. Kalinowski, Acta Phys. Polon. **B30** (1999) 1931.
- [12] J. L. Kneur, G. Moulhacq, *Contribution to the Proceedings of the 4th International Workshop on Linear Colliders (LCWS1999)*, Sitges, Barcelona 1999, hep-ph/9910267.
- [13] J. L. Feng, M. J. Strassler, Phys. Rev. **D55** (1997) 1326;  
J. L. Feng, M. J. Strassler, Phys. Rev. **D51** (1995) 4661.
- [14] G. Moortgat-Pick, H. Fraas, A. Bartl, W. Majerotto, Eur. Phys. J. **C9** (1999) 521.
- [15] S. Y. Choi, A. Djouadi, H. S. Song, P. M. Zerwas, Eur. Phys. J. **C8** (1999) 669.
- [16] C. Blöching, H. Fraas, G. Moortgat-Pick, W. Porod, Eur. Phys. J. **C24** (2002) 297.
- [17] J. L. Feng, Int. J. Mod. Phys. **A13** (1998) 2319.
- [18] C. Blöching, H. Fraas, T. Mayer, G. Moortgat-Pick, WUE-ITP-2001-003, hep-ph/0101176.
- [19] C. Blöching, H. Fraas, LC-TH-2000-017, hep-ph/0001034.
- [20] G. Moortgat-Pick, A. Bartl, H. Fraas, W. Majerotto, LC-TH-2000-033, DESY-00-003, UWThPh-2000-4, WUE-ITP-2000-005, HEPHY-PUB 727/2000, hep-ph/0004181, *and references therein*.

Scenario A		
$M_1 = 76$ GeV	$M_2 = 152$ GeV	$\mu = 316$ GeV
$\tan\beta = 3$	$m_{\tilde{\nu}} = 158$ GeV	$m_0 = 100$ GeV
	$\tilde{\chi}_1^+$	$\tilde{\chi}_1^0$
mass / GeV	128	69.5
mixing	$(W^+ \tilde{H}^+)$ (0.96  - 0.28)	$(\tilde{\gamma} \tilde{Z} \tilde{H}_a \tilde{H}_b)$ (0.78  - 0.59 0.15 0.14)
Scenario B		
$M_1 = 185$ GeV	$M_2 = 370$ GeV	$\mu = 125$ GeV
$\tan\beta = 3$	$m_{\tilde{\nu}} = 339$ GeV	$m_0 = 100$ GeV
	$\tilde{\chi}_1^+$	$\tilde{\chi}_1^0$
mass / GeV	108	91.6
mixing	$(W^+ \tilde{H}^+)$ (0.33  - 0.94)	$(\tilde{\gamma} \tilde{Z} \tilde{H}_a \tilde{H}_b)$ (-0.21 0.37  - 0.78  - 0.47)

Table 1: Masses and mixing character of the light chargino  $\tilde{\chi}_1^\pm$  and the lightest neutralino  $\tilde{\chi}_1^0$  in scenarios A and B.

	Scenario A		Scenario B	
$\sqrt{s_{ee}}/\text{GeV}$	500	800	500	800
$\sigma_e/\text{pb}$	0.09	0.18	0.13	0.19
$A_{\text{FB}}/\%$	-18	-12	0.83	0.36

Table 2: Convolutd cross sections and positron forward-backward asymmetries for  $\gamma\gamma \rightarrow \tilde{\chi}_1^+ \tilde{\chi}_1^-$ ,  $\tilde{\chi}_1^+ \rightarrow \tilde{\chi}_1^0 e^+ \nu_e$  in scenario A and B at  $\sqrt{s_{ee}} = 500$  GeV and  $\sqrt{s_{ee}} = 800$  GeV for polarizations  $(\lambda_{c_1}, \lambda_{L_1}) = (0.85, 0)$ ,  $(\lambda_{c_2}, \lambda_{L_2}) = (-0.85, 0)$ .

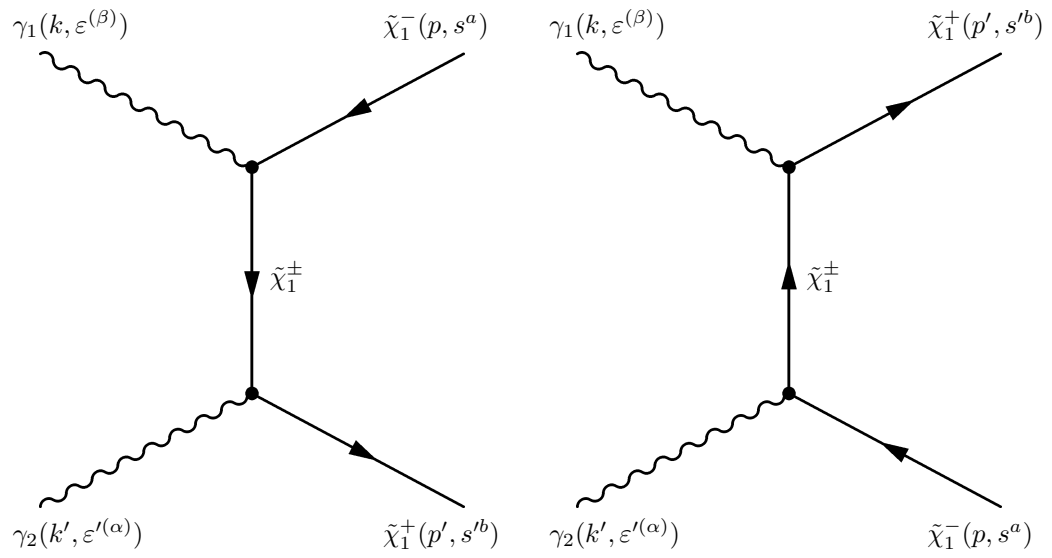


Figure 1: Feynman diagrams for the process  $\gamma_1(k, \varepsilon^{(\beta)}) + \gamma_2(k', \varepsilon'^{(\alpha)}) \rightarrow \tilde{\chi}_1^+(p', s'^b) + \tilde{\chi}_1^-(p, s^a)$

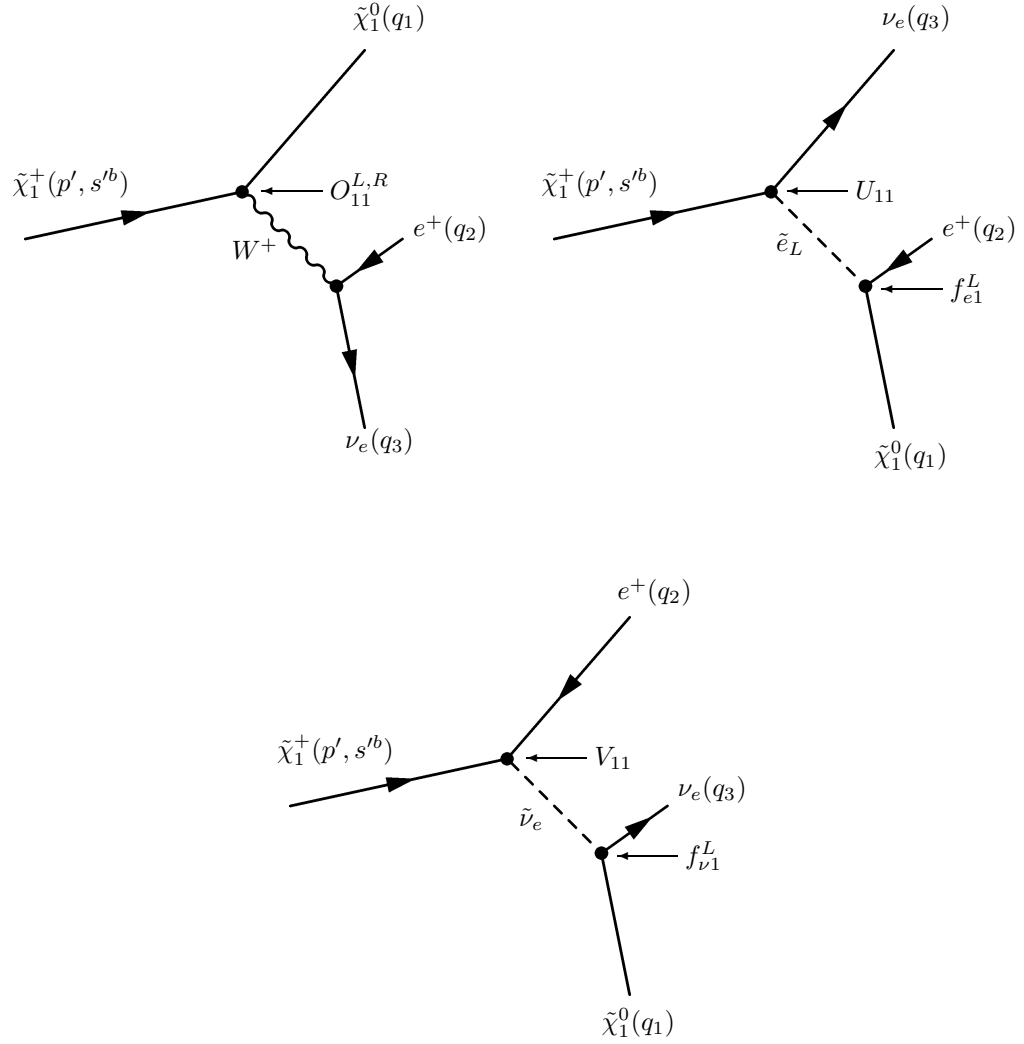


Figure 2: Feynman diagrams for the decay process  $\tilde{\chi}_1^+(p', s^{tb}) \rightarrow \tilde{\chi}_1^0(q_1) + e^+(q_2) + \nu_e(q_3)$ . Couplings as defined in [4].

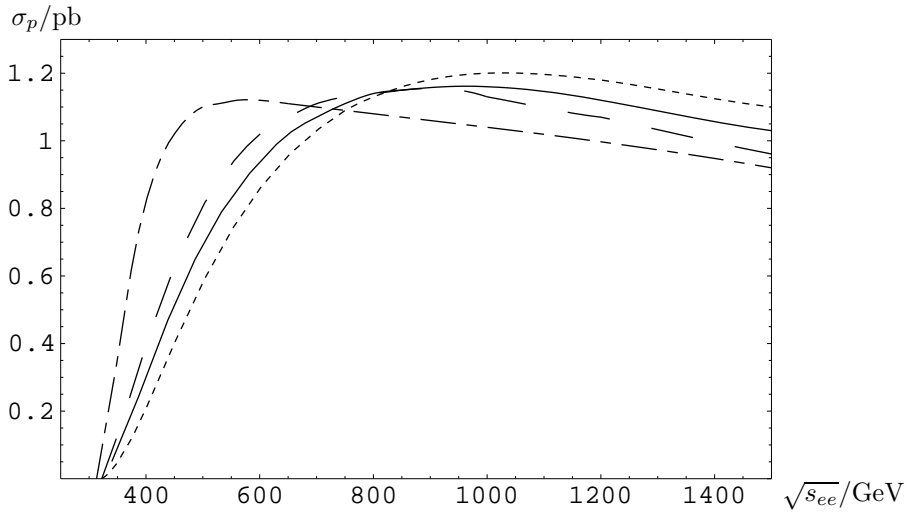


Figure 3: Convoluted cross sections for  $\gamma\gamma \rightarrow \tilde{\chi}_k^+ \tilde{\chi}_k^-$  for  $m_k = 128$  GeV as a function of the ee-CMS energy for polarizations:

- $(\lambda_{c_1}, \lambda_{L_1}) = (0, 0), (\lambda_{c_2}, \lambda_{L_2}) = (0, 0)$  (solid line)
- $(\lambda_{c_1}, \lambda_{L_1}) = (0.85, 0), (\lambda_{c_2}, \lambda_{L_2}) = (-0.85, 0)$  (dashed line)
- $(\lambda_{c_1}, \lambda_{L_1}) = (0.85, 0), (\lambda_{c_2}, \lambda_{L_2}) = (0.85, 0)$  (long-dashed line)
- $(\lambda_{c_1}, \lambda_{L_1}) = (0.85, -1), (\lambda_{c_2}, \lambda_{L_2}) = (0.85, -1)$  (dot-dashed line)



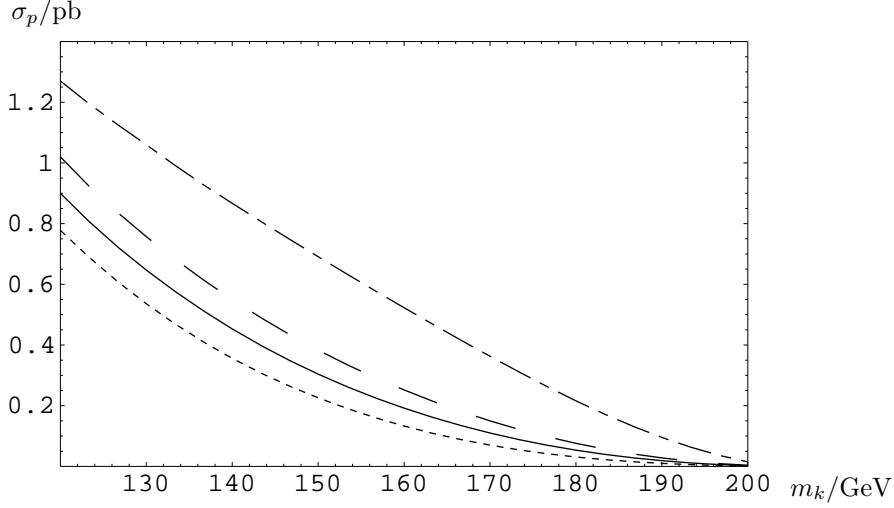


Figure 4: Convoluted cross sections for  $\gamma\gamma \rightarrow \tilde{\chi}_k^+ \tilde{\chi}_k^-$  at  $\sqrt{s_{ee}} = 500$  GeV, as a function of the chargino mass  $m_k$  for polarizations:

- $(\lambda_{c_1}, \lambda_{L_1}) = (0, 0), (\lambda_{c_2}, \lambda_{L_2}) = (0, 0)$  (solid line)
- $(\lambda_{c_1}, \lambda_{L_1}) = (0.85, 0), (\lambda_{c_2}, \lambda_{L_2}) = (-0.85, 0)$  (dashed line)
- $(\lambda_{c_1}, \lambda_{L_1}) = (0.85, 0), (\lambda_{c_2}, \lambda_{L_2}) = (0.85, 0)$  (long-dashed line)
- $(\lambda_{c_1}, \lambda_{L_1}) = (0.85, -1), (\lambda_{c_2}, \lambda_{L_2}) = (0.85, -1)$  (dot-dashed line)

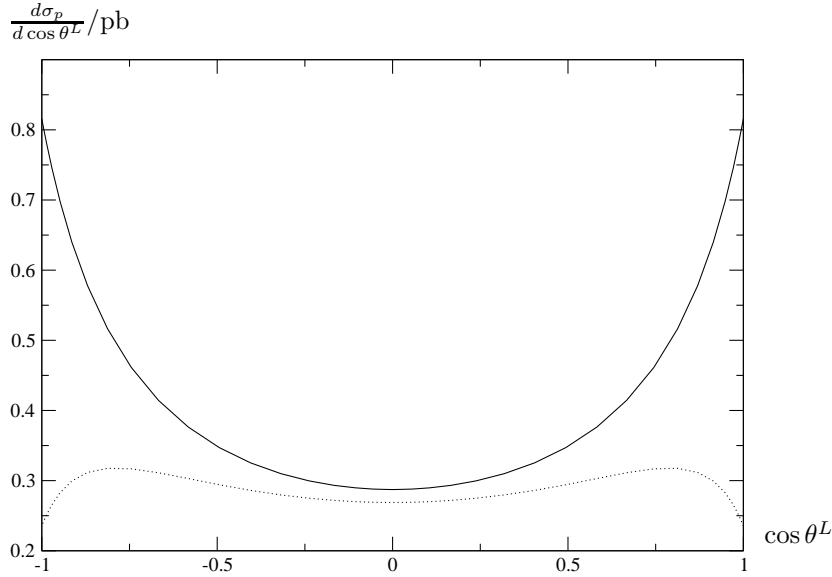


Figure 5: Angular distributions in the ee-CMS for  $\gamma\gamma \rightarrow \tilde{\chi}_k^+ \tilde{\chi}_k^-$  for  $m_k = 128$  GeV and polarizations  $(\lambda_{c_1}, \lambda_{L_1}) = (0.85, 0), (\lambda_{c_2}, \lambda_{L_2}) = (0.85, 0)$  (solid line),  $(\lambda_{c_1}, \lambda_{L_1}) = (0.85, 0), (\lambda_{c_2}, \lambda_{L_2}) = (-0.85, 0)$  (dotted line) at  $\sqrt{s_{ee}} = 500$  GeV.

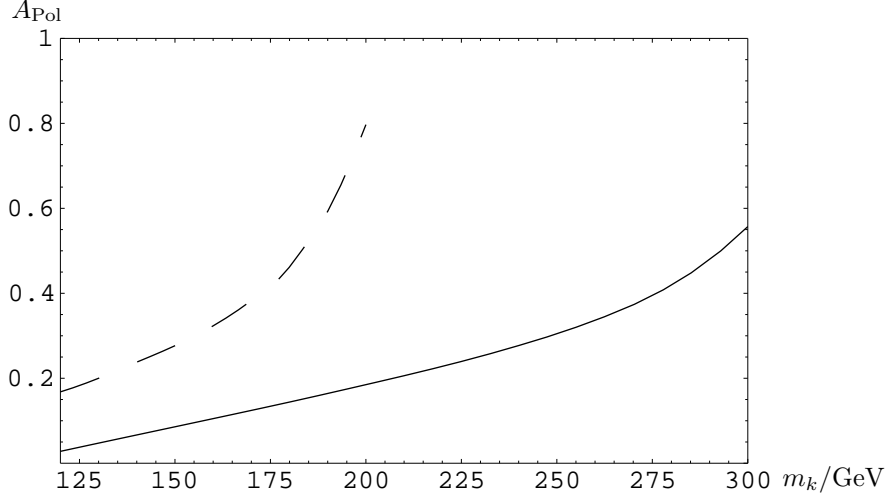


Figure 6: Polarization asymmetry (defined in (46)) of the convoluted cross section  $\gamma\gamma \rightarrow \tilde{\chi}_k^+ \tilde{\chi}_k^-$  as a function of the chargino mass  $m_k$  for polarizations  $(\lambda_{c_1}, \lambda_{L_1}) = (0.85, 1)$ ,  $(\lambda_{c_2}, \lambda_{L_2}) = (-0.85, \pm 1)$  at  $\sqrt{s_{ee}} = 500$  GeV corresponding to  $\sqrt{s_{\gamma\gamma}^{max}} = 415$  GeV (dashed line) and  $\sqrt{s_{ee}} = 800$  GeV corresponding to  $\sqrt{s_{\gamma\gamma}^{max}} = 664$  GeV (solid line).

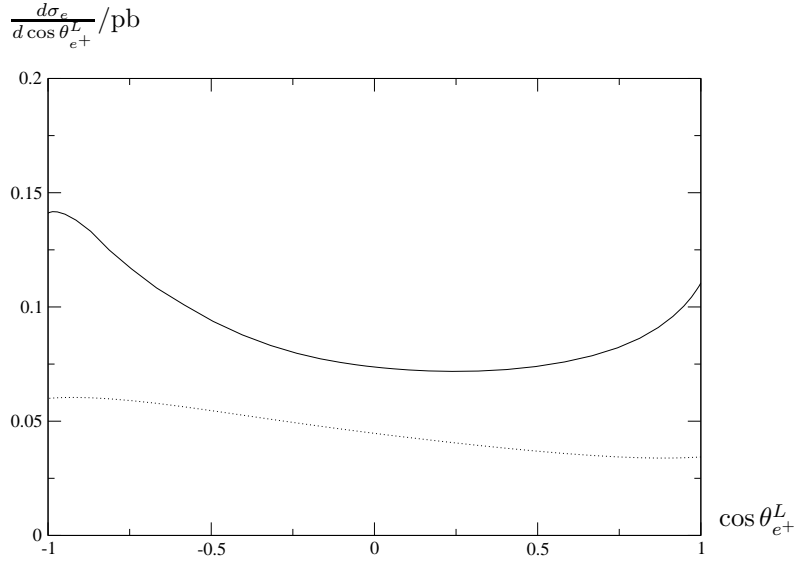


Figure 7: Angular distribution in the ee-CMS of the decay positron in  $\gamma\gamma \rightarrow \tilde{\chi}_1^+ \tilde{\chi}_1^-$ ,  $\tilde{\chi}_1^+ \rightarrow \tilde{\chi}_1^0 e^+ \nu_e$  for scenario A and polarizations  $(\lambda_{c_1}, \lambda_{L_1}) = (0.85, 0)$ ,  $(\lambda_{c_2}, \lambda_{L_2}) = (-0.85, 0)$  at  $\sqrt{s_{ee}} = 500$  GeV (dotted line) and  $\sqrt{s_{ee}} = 800$  GeV (solid line).

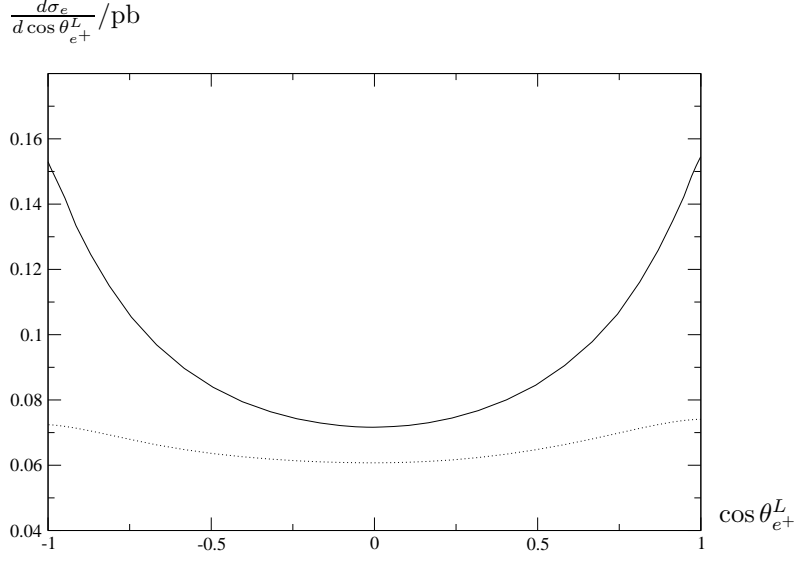


Figure 8: Angular distribution in the ee-CMS of the decay positron in  $\gamma\gamma \rightarrow \tilde{\chi}_1^+ \tilde{\chi}_1^-$ ,  $\tilde{\chi}_1^+ \rightarrow \tilde{\chi}_1^0 e^+ \nu_e$  for scenario B and polarizations  $(\lambda_{c_1}, \lambda_{L_1}) = (0.85, 0)$ ,  $(\lambda_{c_2}, \lambda_{L_2}) = (-0.85, 0)$  at  $\sqrt{s_{ee}} = 500$  GeV (dotted line) and  $\sqrt{s_{ee}} = 800$  GeV (solid line).

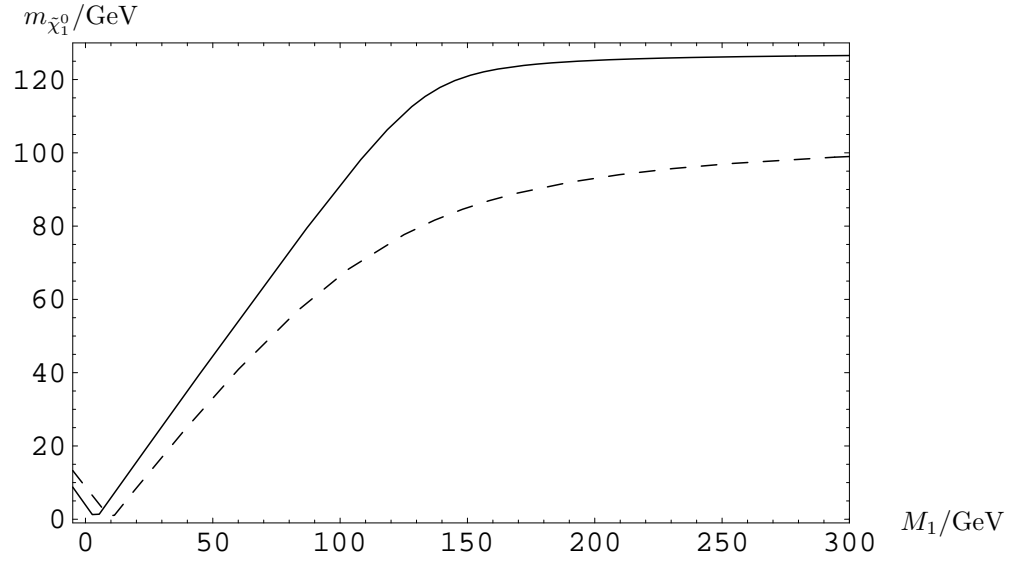


Figure 9:  $M_1$ -dependence of the LSP mass for  $M_2 = 152$  GeV,  $\mu = 316$  GeV,  $\tan \beta = 3$  (solid line) and for  $M_2 = 370$  GeV,  $\mu = 125$  GeV,  $\tan \beta = 3$  (dashed line).

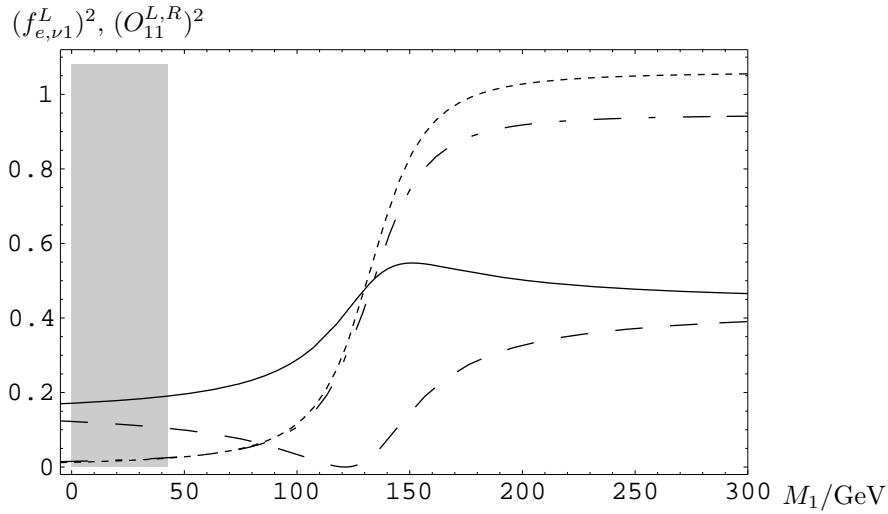


Figure 10:  $M_1$ -dependence of the couplings  $(f_{\nu 1}^L)^2$  (solid line),  $(f_{e 1}^L)^2$  (dashed line),  $(O_{11}^L)^2$  (long-dashed line) and  $(O_{11}^R)^2$  (dot-dashed line) as defined in [4] for  $M_2 = 152$  GeV,  $\mu = 316$  GeV,  $\tan \beta = 3$  (corresponding to scenario B). The shadowed region is excluded by the lower bound  $m_{\tilde{\chi}_1^0} > 38$  GeV.

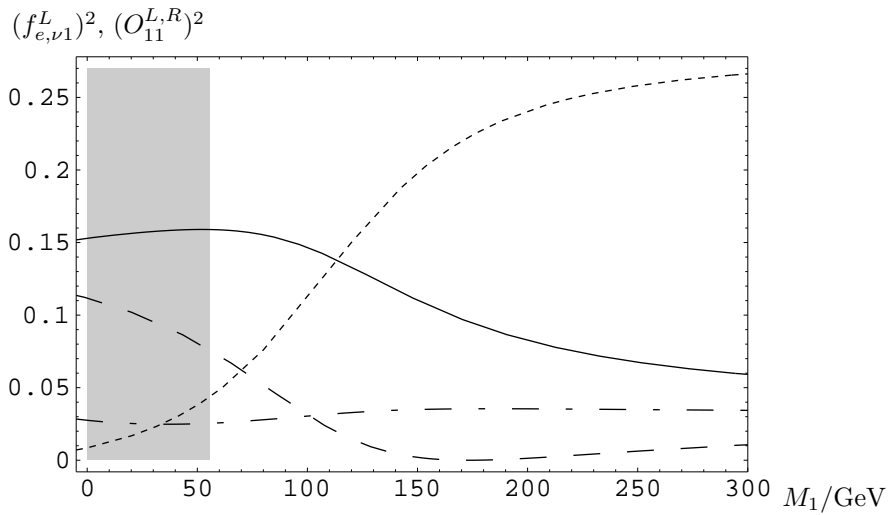


Figure 11:  $M_1$ -dependence of the couplings  $(f_{\nu 1}^L)^2$  (solid line),  $(f_{e 1}^L)^2$  (dashed line),  $(O_{11}^L)^2$  (long-dashed line) and  $(O_{11}^R)^2$  (dot-dashed line) as defined in [4] for  $M_2 = 370$  GeV,  $\mu = 125$  GeV,  $\tan \beta = 3$  (corresponding to scenario B). The shadowed region is excluded by the lower bound  $m_{\tilde{\chi}_1^0} > 38$  GeV.

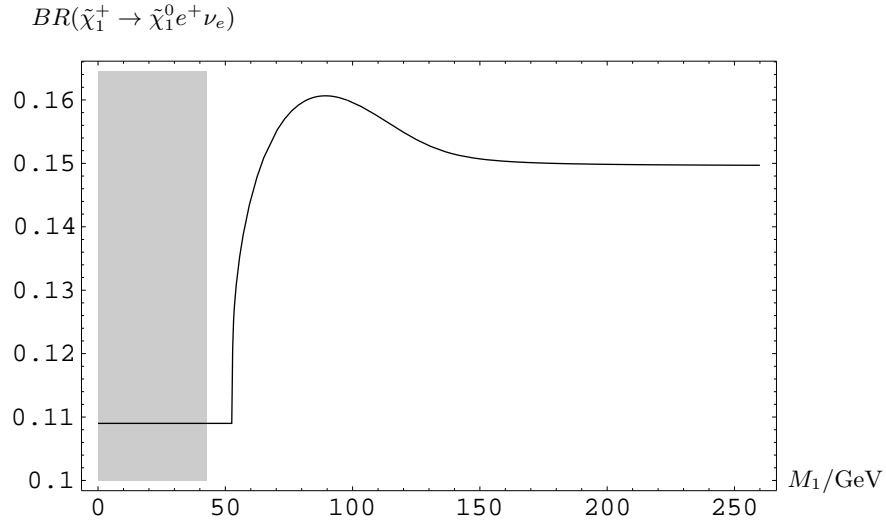


Figure 12: Branching ratio for  $\tilde{\chi}_1^+ \rightarrow \tilde{\chi}_1^0 e^+ \nu_e$  as a function of the parameter  $M_1$  for  $M_2 = 152$  GeV,  $\mu = 316$  GeV,  $\tan \beta = 3$ . The shadowed region is excluded by the lower bound  $m_{\tilde{\chi}_1^0} > 38$  GeV.

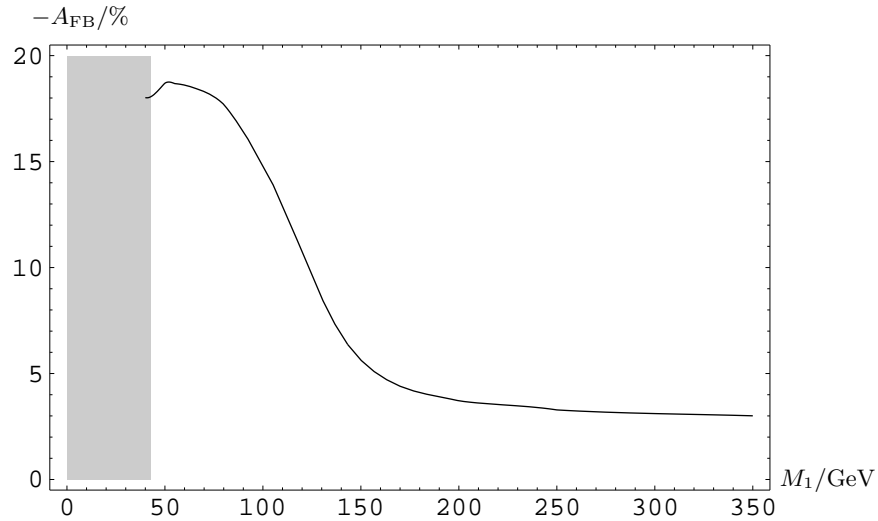


Figure 13: Forward-backward asymmetry in the ee-CMS of the decay positron from  $\gamma\gamma \rightarrow \tilde{\chi}_1^+ \tilde{\chi}_1^-$ ,  $\tilde{\chi}_1^+ \rightarrow \tilde{\chi}_1^0 e^+ \nu_e$  as a function of the parameter  $M_1$  at  $\sqrt{s_{ee}} = 500$  GeV for  $(\lambda_{c_1}, \lambda_{L_1}) = (0.85, 0)$ ,  $(\lambda_{c_2}, \lambda_{L_2}) = (-0.85, 0)$  for  $M_2 = 152$  GeV,  $\mu = 316$  GeV,  $\tan \beta = 3$ . The shadowed region is excluded by the lower bound  $m_{\tilde{\chi}_1^0} > 38$  GeV.

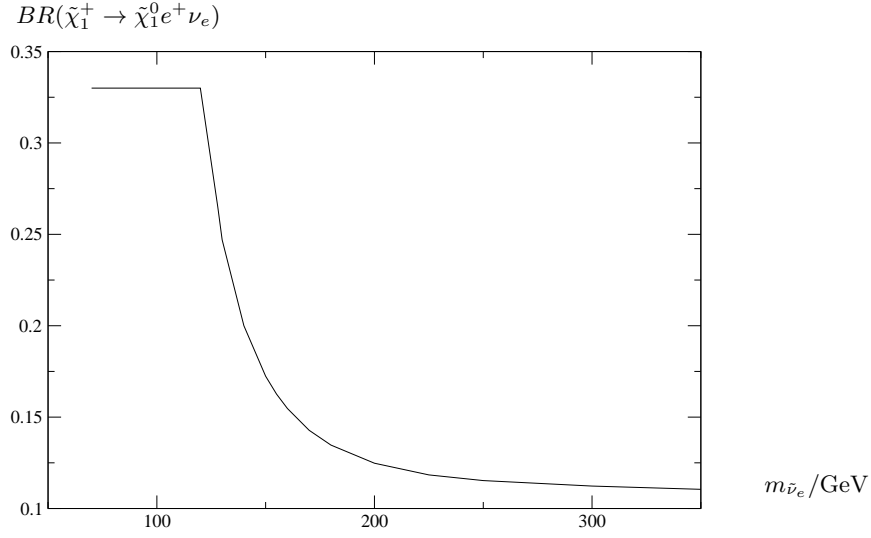


Figure 14: Branching ratio for  $\tilde{\chi}_1^+ \rightarrow \tilde{\chi}_1^0 e^+ \nu_e$  as a function of the sneutrino mass  $m_{\tilde{\nu}_e}$  for  $M_2 = 152$  GeV,  $\mu = 316$  GeV,  $\tan \beta = 3$ .

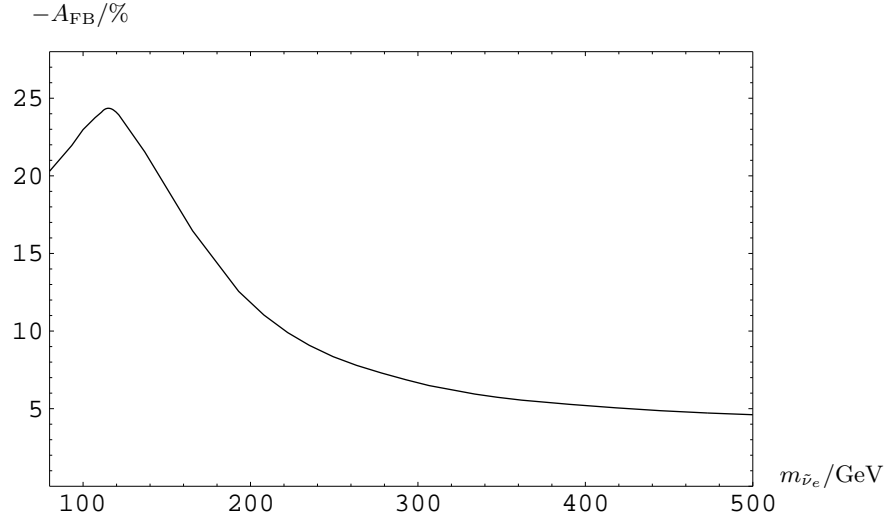


Figure 15: Forward-backward asymmetry in the ee-CMS of the decay positron from  $\gamma\gamma \rightarrow \tilde{\chi}_1^+ \tilde{\chi}_1^-$ ,  $\tilde{\chi}_1^+ \rightarrow \tilde{\chi}_1^0 e^+ \nu_e$  as a function of the sneutrino mass  $m_{\tilde{\nu}_e}$  at  $\sqrt{s_{ee}} = 500$  GeV for  $(\lambda_{e_1}, \lambda_{L_1}) = (0.85, 0)$ ,  $(\lambda_{e_2}, \lambda_{L_2}) = (-0.85, 0)$  for  $M_2 = 152$  GeV,  $\mu = 316$  GeV,  $\tan \beta = 3$ .